Direct Lightning Surge Analysis of Distribution Lines Considering LEMPs From Lightning Channel and Struck Pole in EMT Simulation

Akifumi Yamanaka, *Member, IEEE*, Kazuyuki Ishimoto, *Member, IEEE*, and Akiyoshi Tatematsu, *Senior Member, IEEE*

***Abstract*—Direct lightning strikes mainly determine the lightning performance of medium-voltage distribution lines with surge arresters installed at close intervals. Recent studies have shown that in such lines, the effect of a lightning electromagnetic pulse (LEMP) on insulator voltages has a large impact on lightning performance assessment. In this article, we propose an analysis method that can consider the effect of LEMPs radiated from the lightning channel and the struck pole in electromagnetic transient (EMT) analysis. In the proposed method, first, the LEMPs are calculated using potential formulae that are extended to include the presence of the struck pole. Second, the insulator voltages induced by the LEMPs and generated by currents flowing into the struck pole, earth electrode, and shield wire are calculated using a field-to-line coupling formula interfaced with the EMT analysis. The proposed method is validated by comparison with three-dimensional finite-difference time-domain analysis. The proposed method is potentially a powerful tool for statistically assessing the lightning performance of distribution lines while considering LEMP effects.**

***Index Terms*—Electromagnetic transient (EMT) analysis, field-to-line coupling formula, lightning electromagnetic pulse (LEMP), lightning, medium-voltage distribution line.**

I. Introduction

DIRECT and indirect lightning cause outages in medium-voltage (MV) distribution lines. The number of indirect lightning strikes is much larger than that of direct lightning strikes, and the main concern in the flashover analysis of MV distribution lines is usually indirect lightning strikes [1], [2]. However, in well-protected distribution lines with surge arresters installed at close intervals and periodically grounded shield wires, indirect lightning rarely causes outages [3]. Thus, direct lightning strikes are the main concern in lightning surge analysis and in discussing countermeasures, especially for well-protected distribution lines [4], [5], [6], [7], [8].

Direct lightning strikes to distribution lines have long been analyzed by electromagnetic transient (EMT) simulators. In the analysis, the lightning has been simply represented by a current source in parallel with an equivalent lightning channel impedance (constant resistance); the effect of a lightning electromagnetic pulse (LEMP) on overhead conductors has been neglected [5], [6], [7], [8], [9], [10], [11]. This is because the voltage rise due to the effect of LEMPs is assumed to be much lower than that due to the current flowing into the struck pole and shield wires.

However, recent studies [12], [13], [14], [15], [16] have shown the LEMP effect on insulator voltages. In particular, Ishimoto et al. [15] demonstrated the significant effect of LEMPs on insulator voltages by comparing EMT analysis using electromagnetic transients program (EMTP) [17], which neglects the LEMP effect, and full-wave three-dimensional finite-difference time-domain (3-D FDTD) [18] analysis using virtual surge test lab restructured and extended version (VSTL REV) [19], which inherently and accurately considers the LEMP effect. Owing to the LEMP effect, insulator voltages are about two times higher in the first stroke and 1.3 times higher in the subsequent stroke than those without the LEMP effect.

Moreover, a method that approximately considers the LEMP effect in EMT analysis using the lightning-induced overvoltage (LIOV)-EMTP code [20], [21] has been confirmed to provide voltages similar to those obtained by the FDTD method [15]. The use of the LIOV-EMTP code enables the LEMP effect to be considered in EMT analysis. Therefore, the method provides a practical tool for statistically evaluating the lightning performance of distribution lines owing to its computation time being shorter than that of full-wave analysis while providing computed voltages as accurate as those computed by full-wave analysis.

Although the LIOV-EMTP-based method provides similar voltages to the 3-D FDTD method and hence is quite practical, as shown in Fig. 1, the method computes LEMPs assuming a lightning strike to flat ground 10 m from the pole and superimposes the voltage induced by the LEMPs on the voltages derived by conventional EMT analysis (with the lightning current injected at the top of the pole model). Lightning-induced voltage analysis programs cannot model a direct lightning strike to distribution poles since they assume a lightning strike to flat ground away from distribution lines.

Another method for considering the LEMPs in a direct lightning strike in EMT analysis was presented in [22] and [23].

Manuscript received 23 December 2022; revised 19 May 2023; accepted 21 September 2023. Date of publication 9 October 2023; date of current version 13 December 2023. *(Corresponding author: Akifumi Yamanaka.)*

The authors are with the Central Research Institute of Electric Power Industry, Yokosuka-shi 240-0196, Japan (e-mail: yamanaka3929@criepi.denken.or.jp; ishimoto@criepi.denken.or.jp; akiyoshi@criepi.denken.or.jp).

Color versions of one or more figures in this article are available at https://doi.org/10.1109/TEMC.2023.3319032.

Digital Object Identifier 10.1109/TEMC.2023.3319032

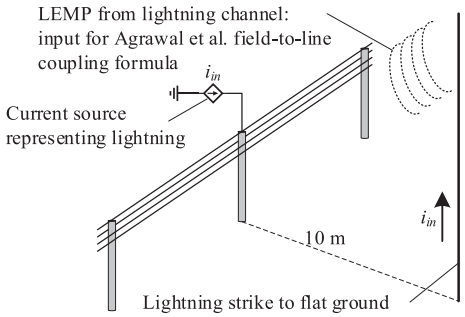

Fig. 1. Concept of lightning surge analysis method used by Ishimoto et al. [15]. A lightning strike to flat ground 10 m from the struck pole is assumed in LEMP calculation.

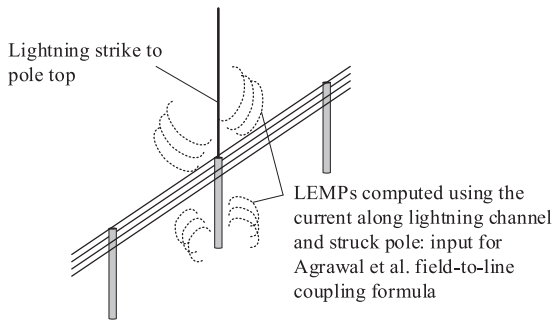

Fig. 2. Concept of proposed lightning surge analysis method: LEMPs from the lightning channel and the struck pole are computed from the current distribution, and their effect on overhead conductors is computed using the Agrawal et al. field-to-line coupling formula.

In this method, the LEMP effect was considered on the basis of the Rusck model, and it was applied to analyze a direct lightning strike to a transmission line. Although this method can consider the LEMP caused by a return stroke current as well as the lightning strike point correctly unlike the aforementioned LIOV-EMTP-based method, it did not include the effect of LEMPs from the struck object (a transmission tower in these studies).

In this article, we propose an EMT-based analysis method for a direct lightning strike to distribution lines that considers the LEMPs radiated from the lightning channel and the pole struck by lightning, and we discuss the effect of an LEMP on the insulator voltages of a distribution line struck by lightning. In the proposed method, the scalar and vector potential formulae presented in [24] are extended to include the presence of the struck pole in the LEMP calculation. The Agrawal et al. field-to-line coupling formula [25] is used to compute the voltages induced on overhead conductors.

The rest of the article is organized as follows. Section II presents the methodology of the computation: the potential method for computing the LEMPs from the lightning channel and the struck pole, the FDTD method for solving the Agrawal et al. formula, and the interface of the coupling formula with the EMT analysis. Section III gives a comparison of insulator voltages computed by the proposed method, the 3-D FDTD method using VSTL REV, and EMT analysis without considering LEMPs. Section IV concludes this article. Appendix A provides a validation of the proposed method, taking as an example the calculation of the induced voltage by the lightning strike to a tall object located near an overhead conductor. Appendix B discusses the method assuming a lightning strike to flat ground 10 m from the struck pole.

II. Methodology

A. Concept and Overview of Proposed Method

The proposed method explicitly represents the direct lightning strike to the distribution pole and considers the LEMP effect from the channel as well as the struck pole, as shown in Fig. 2. Note that the LEMP effect from the current flowing into the shield wire is considered by the mutual coupling in the Agrawal et al. formula. The analysis program is based on EMT analysis with the following three additional calculation parts:

1) calculating the current along the lightning channel and the struck pole;
2) calculating the LEMP;
3) solving the Agrawal et al. formula interfaced with EMT analysis.

The proposed method is based on EMT analysis since it enables us to perform lightning surge analysis with various models, such as distribution poles, grounding resistance, insulator flashovers, surge arresters, pole-mounted transformers, and others with a small computational load. In the EMT analysis part, the sparse tableau method is used to compose a conductance matrix [26], and a transient response is derived using the trapezoidal rule for numerical integration [27].

The rest of this section describes the three additional calculation parts. Section II-B covers the part for calculating the current along the lightning channel and the struck object, Section II-C covers the LEMP calculation part, and Section II-D covers the part for solving the Agrawal et al. formula and the interface of this formula with EMT analysis.

B. Calculation of Currents Along Lightning Channel and Struck Pole

The LEMPs are calculated by considering a current traveling upward along the lightning channel, i_{ch}, and currents traveling downward and upward along the struck pole, i_d, and i_u, respectively. These currents are derived from the branch currents in the EMT analysis shown in Fig. 3. The current traveling upward along the lightning channel, i_{ch}, can be calculated from the lightning short-circuit current i_{sc} and the current flowing into the equivalent lightning channel impedance, $i_{R\mathrm{ch}}$, as follows:

$$i_{\mathrm{ch}}(t) = i_{\mathrm{sc}}(t) + i_{R_{\mathrm{ch}}}(t). \tag{1}$$

The current traveling downward along the pole struck by lightning, i_d, can be calculated from the total current at the pole top, i_t, and the current source holding history at the pole base of Dommel's distribution line model [27], J_t, as follows:

$$i_d(t) = i_t(t) - J_t(t)/2. \tag{2}$$

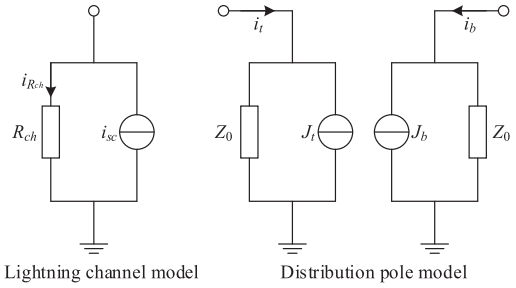

Fig. 3. Models of lightning channel and distribution pole in the EMT analysis and definition of branch currents to used derive i_{ch}, i_d, and i_u (see Fig. 5).

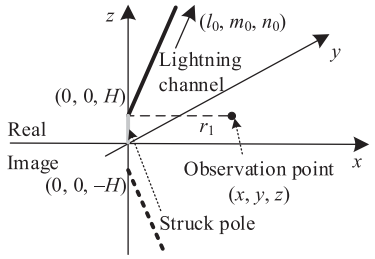

Fig. 4. Lightning channel and its image for computing scalar and vector potentials at observation point (x, y, z).

In the same manner, the current traveling upward along the pole struck by lightning, i_u, can be calculated as follows:

$$i_u(t) = -\left[i_b(t) - J_b(t)/2\right] \tag{3}$$

where i_b is the total current at the base of the struck pole and J_b is the current source holding history at the pole top.

C. LEMP Calculation by Potential Method

1) Basic Formula: The electric fields required in the Agrawal et al. formula are calculated from the scalar and vector potentials. The following is assumed in the calculation [24].

1) The charge distribution along the leader is uniform.
2) The current waveform is given by a step function.
3) The return stroke speed is constant.
4) The current along the lightning channel does not suffer attenuation or distortion.

The potential formula is also used to compute LEMPs radiated from the distribution pole struck by lightning.

A unit step charge traveling from point $(0, 0, h)$ at a constant speed v generates a scalar potential at point (x, y, z), as shown in Fig. 4, as follows:

$$\phi = \frac{1}{4\pi\varepsilon_0 v} \ln \frac{vt - \xi_1 + \sqrt{(vt-\xi_1)^2 + (1-\beta^2)(r_1^2 - \xi_1^2)}}{(1+\beta)(r_1 - \xi_1)} \tag{4}$$

where ε_0 is the permittivity in free space and β is the ratio of the speed v to the speed of light in free space, c_0. Variables r_1 and ξ_1 are given as follows:

$$r_1 = \sqrt{x^2 + y^2 + (z-h)^2}, \tag{5}$$

$$\xi_1 = l_0 x + m_0 y + n_0 (z - h) \tag{6}$$

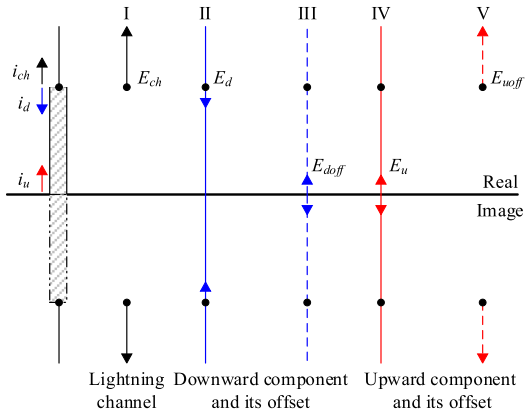

Fig. 5. Conceptual figure for computing LEMPs from lightning channel and pole struck by lightning.

where l_0, m_0, and n_0 are the direction cosines of the channel. The image charge generates the following scalar potential:

$$\phi' = \frac{-1}{4\pi\varepsilon_0 v} \ln \frac{vt - \xi_2 + \sqrt{(vt-\xi_2)^2 + (1-\beta^2)(r_2^2 - \xi_2^2)}}{(1+\beta)(r_2 - \xi_2)} \tag{7}$$

where

$$r_2 = \sqrt{x^2 + y^2 + (z+h)^2}, \tag{8}$$

$$\xi_2 = l_0 x + m_0 y - n_0 (z + h). \tag{9}$$

The total scalar potential ϕ_s is given by the sum of the real and image potentials with an appropriate time delay

$$\phi_s = \phi u(t - r_1/c_0) + \phi' u(t - r_2/c_0) \tag{10}$$

where $u(t)$ is Heaviside's step function.

The real vector potential $\boldsymbol{A}$ generated by a unit step current can be derived using a unit vector of the current, $\boldsymbol{i}$, in the same manner as the scalar potential

$$\boldsymbol{A} = \boldsymbol{i}\frac{\mu_0}{4\pi} \ln \frac{vt - \xi_1 + \sqrt{(vt-\xi_1)^2 + (1-\beta^2)(r_1^2 - \xi_1^2)}}{(1+\beta)(r_1 - \xi_1)}. \tag{11}$$

The image vector potential can also be derived similarly to the scalar potential.

Using the total scalar and vector potentials, the electric field at an arbitrary point can be derived as follows:

$$\boldsymbol{E} = -\nabla\phi_s - \frac{\partial \boldsymbol{A_v}}{\partial t} \tag{12}$$

where $\boldsymbol{A_v}$ is the total vector potential.

2) Inclusion of Pole Struck by Lightning: The pole struck by lightning is incorporated by the superimposition of the electric field calculation in the previous section. Fig. 5 shows the concept of the proposed method. The electric field generated by the current along the lightning channel is calculated from (12). In representing the electric fields from the struck pole, the field generated by the downward current and its offset, and the field generated by the upward current and its offset are used. As shown

in Fig. 5, the offsets cancel redundant fields: the potential method assumes a unit step charge (current) traveling a semi-infinite length from the initial point, as described in Section II-C1. Consequently, the total electric field is calculated by superimposing the following five components:

1) $E_{\rm ch}$: field generated by the current along the lightning channel, $i_{\rm ch}$.
2) E_d: field generated by the current traveling downward along the struck object, i_d.
3) $E_{d\rm off}$: field that cancels the redundant term of E_d (offset of E_d).
4) $E_{\rm u}$: field generated by the current traveling upward along the struck object, i_u.
5) $E_{u\rm off}$: field that cancels the redundant term of E_u (offset of E_u).

The calculation of each field is further described in Section II-C2 (a)–(e). Note that although this article focuses on the electric field radiation from the lightning channel and the struck pole, the proposed method for the struck pole can also be used for the calculation of the electric field from the nearby poles.

a) E_{ch}: Field generated by current along lightning channel: Hereafter, the formulae of the horizontal electric field derived from scalar and vector potentials by (12) for the aforementioned five components are shown.

The field $E_{\rm ch}$ is generated by the lightning channel. For simplicity, the direction cosine l_0 and m_0 are set to 0, and n_0 is set to 1; a vertical channel is assumed. The field generated by an arbitrary channel current can be derived as follows:

$$E_{\rm ch}(t) = [E_{\rm chRe}(t) - E_{\rm chIm}(t)] * i_{ch}(t) \tag{13}$$

where $*$ denotes the convolution integral, and each electric field component is given by the following formulae:

$$E_{\rm chRe}(t) = E_x(t, r_{\rm chRe}, \xi_{\rm chRe}, v, \beta), \tag{14}$$

$$E_{\rm chIm}(t) = E_x(t, r_{\rm chIm}, \xi_{\rm chIm}, v, \beta), \tag{15}$$

$$E_x(t, r, \xi, v, \beta) = \frac{1}{4\pi\varepsilon_0 v\beta} u\left(t - \frac{r}{c_0}\right)\left[\frac{(1-\beta^2)(x-x_0)}{\chi(vt-\xi+\chi)} - \frac{x-x_0}{r(r-\xi)}\right],$$

$$\chi = \sqrt{(vt-\xi)^2 + (1-\beta^2)(r^2-\xi^2)} \tag{16}$$

$$r_{\rm chRe} = r_1,\ r_{\rm chIm} = r_2, \tag{17}$$

$$\xi_{\rm chRe} = z - h,\ \xi_{\rm chIm} = -(z+h). \tag{18}$$

Although the vertical channel is assumed here, the potential formulae can represent an inclined channel by setting l_0, n_0, and m_0 to specific values and even a tortuous channel by superimposition [24]. Since the Agrawal et al. formula that considers the contribution of the vector potential to the horizontal electric field [25], [28] is used to compute induced voltages, inclined and tortuous channels can be analyzed by the proposed method.

b) E_d: Field generated by current traveling downward along struck object: The field E_d is derived from the formulae shown below. Here, the current traveling speed is assumed to be the light speed in free space, c_0 (this is a general assumption for distribution poles). With this assumption, the step response of the electric field can be expressed by a step function: the convolution integral for deriving an arbitrary current response becomes a product

$$\begin{aligned} E_d(t) &= [E_{d\rm Re}(t) - E_{d\rm Im}(t)] * i_d(t) \\ &= E_{d\rm Re}(t)\, i_d(t - r_{d\rm Re}/c_0) \\ &\quad - E_{d\rm Im}(t)\, i_d(t - r_{d\rm Im}/c_0) \end{aligned} \tag{19}$$

$$E_{d\rm Re}(t) = E_{xst}(t, r_{d\rm Re}, \xi_{d\rm Re}) \tag{20}$$

$$E_{d\rm Im}(t) = E_{xst}(t, r_{d\rm Im}, \xi_{d\rm Im}) \tag{21}$$

$$E_{xst}(t, r, \xi) = \frac{1}{4\pi\varepsilon_0 c_0}\frac{x-x_0}{r(r-\xi)} u\left(t - \frac{r}{c_0}\right) \tag{22}$$

$$r_{d\rm Re} = r_{ch\rm Re},\ r_{d\rm Im} = r_{ch\rm Im} \tag{23}$$

$$\xi_{d\rm Re} = \xi_{\rm chIm},\ \xi_{d\rm Im} = \xi_{\rm chRe}. \tag{24}$$

This field produces the redundant components located below and above the pole in the image and real regions, respectively, as shown in Fig. 5(II). Hence, the field $E_{d\rm off}$, which cancels these redundant components, is required.

c) E_{doff}: Offset of E_d: The field $E_{d\rm off}$ cancels the redundant components generated by E_d, as shown in Fig. 5(III). The starting point of $E_{d\rm off}$ is the base of the pole, and $E_{d\rm off}$ is calculated by considering the traveling time delay t_p ($= h/c_0$, where h is the height of the struck pole) along the pole

$$\begin{aligned} E_{d\rm off}(t) &= [E_{d\rm offRe}(t-t_p) - E_{d\rm offIm}(t-t_p)] * i_d(t-t_p) \\ &= [E_{d\rm offRe}(t-t_p) - E_{d\rm offIm}(t-t_p)] \\ &\quad i_d(t - t_p - r_{d\rm off}/c_0) \end{aligned} \tag{25}$$

$$E_{d\rm offRe}(t) = E_{xst}(t, r_{d\rm offRe}, \xi_{d\rm offRe}) \tag{26}$$

$$E_{d\rm offIm}(t) = E_{xst}(t, r_{d\rm offIm}, \xi_{d\rm offIm}) \tag{27}$$

$$r_{d\rm offRe} = r_{d\rm offIm} = r_{d\rm off} = \sqrt{x^2+y^2+z^2} \tag{28}$$

$$\xi_{d\rm offRe} = z,\ \xi_{d\rm offIm} = -z. \tag{29}$$

d) E_u: Field generated by current traveling upward along struck object: The starting point of the field E_u is at the base of the pole, as shown in Fig. 5(III). The field is calculated by considering the traveling time delay t_p as follows:

$$\begin{aligned} E_u(t) &= [E_{u\rm Re}(t-t_p) - E_{u\rm Im}(t-t_p)] * i_u(t) \\ &= [E_{u\rm Re}(t-t_p) - E_{u\rm Im}(t-t_p)]\, i_u(t - r_u/c_0), \end{aligned} \tag{30}$$

$$E_{u\rm Re}(t) = E_{xst}(t, r_{u\rm Re}, \xi_{u\rm Re}), \tag{31}$$

$$E_{u\rm Im}(t) = E_{xst}(t, r_{u\rm Im}, \xi_{u\rm Im}), \tag{32}$$

$$r_{u\rm Re} = r_{u\rm Im} = r_u = r_{d\rm off}, \tag{33}$$

$$\xi_{u\rm Re} = z,\ \xi_{u\rm Im} = -z. \tag{34}$$

This field produces the redundant components located above the pole in the real region and below the pole in the image region, as shown in Fig. 5(IV). Hence, the field $E_{u\text{off}}$, which cancels these redundant components, is required.

e) E_{uoff}: Offset of E_u: The field $E_{u\text{off}}$ cancels the redundant components generated by E_u, as shown in Fig. 5(V). The starting point of $E_{u\text{off}}$ is the top of the pole, and $E_{u\text{off}}$ is calculated by considering the round-trip traveling time delay of $2t_p$

$$\begin{aligned} E_{u\text{off}}(t) = & -\left[E_{u\text{offRe}}(t-2t_p) - E_{u\text{offIm}}(t-2t_p)\right] * \\ & i_u(t-t_p) \\ = & -E_{u\text{offRe}}(t-2t_p)\, i_u(t-t_p-r_{u\text{offRe}}/c_0) \\ & + E_{u\text{offIm}}(t-2t_p)\, i_u(t-t_p-r_{u\text{offIm}}/c_0) \end{aligned} \tag{35}$$

$$E_{u\text{offRe}}(t) = E_{xst}(t, r_{u\text{offRe}}, \xi_{u\text{offRe}}) \tag{36}$$

$$E_{u\text{offIm}}(t) = E_{xst}(t, r_{u\text{offIm}}, \xi_{u\text{offIm}}) \tag{37}$$

$$r_{u\text{offRe}} = r_{\text{chRe}},\ r_{u\text{offIm}} = r_{\text{chIm}} \tag{38}$$

$$\xi_{u\text{offRe}} = \xi_{\text{chIm}},\ \xi_{u\text{offIm}} = \xi_{\text{chRe}}. \tag{39}$$

D. Agrawal et al. Field-to-Line Coupling Formula and its Interface With EMT Analysis

1) Basic Formula: The Agrawal et al. field-to-line coupling formula [25] is used to compute the voltages induced on overhead conductors by the LEMPs from the lightning channel and the struck pole. The formula for a lossless single-conductor system is

$$\begin{aligned} & \frac{\partial v^s(x,t)}{\partial x} + L'\frac{\partial i(x,t)}{\partial t} + \int_0^t \xi_g(t-\tau)\frac{\partial i(x,t)}{\partial t}\mathrm{d}\tau \\ & = E_x^i(x,h,t), \end{aligned} \tag{40}$$

$$\frac{\partial i(x,t)}{\partial x} + C'\frac{\partial v^s(x,t)}{\partial t} = 0 \tag{41}$$

where v^s and i are the scattered voltage and total current; x, h, and t are the line position, line height, and time; L' and C' are the line inductance and capacitance; and E_x^i and ξ_g are the incident horizontal electric field and ground impedance, respectively. The total voltage v^t is calculated by considering the incident voltage v^i which is derived from the incident vertical electric field E_z^i as follows:

$$\begin{aligned} v^t(x,t) = v^s(x,t) + v^i(x,t) = v^s(x,t) \\ - \int_0^h E_z^i(x,z,t)\,\mathrm{d}z. \end{aligned} \tag{42}$$

The integral of (42) is calculated by using the trapezoidal rule: the approximation $v^i(x,t) = hE_z^i(x,0,t)$ is not valid in the vicinity of the lightning channel and the struck pole.

The approximation formulae [29], [30] are used to consider the ground impedance. The frequency-partitioning fitting technique is applied to the ground impedance, and the effect of impedance is implemented in the EMT analysis by using the trapezoidal rule [31], [32]. Hence, (40) can be rewritten as follows:

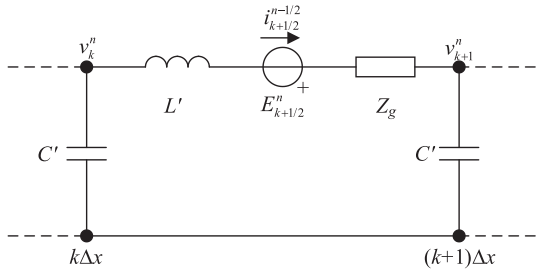

Fig. 6. Voltage and current allocations in the FDTD method for solving Agrawal et al. formula. Z_g indicates the transient ground impedance.

$$\begin{aligned} & \frac{\partial v^s(x,t)}{\partial x} + L'\frac{\partial i(x,t)}{\partial t} + H_0 i(x,t) + x'(x,t) \\ & = E_x^i(x,h,t), \end{aligned} \tag{43}$$

where

$$H_0 = \sum_{m=1}^{M_r} A_m + 2\sum_{m=1}^{M_c} \mathrm{Re}\{B_m\}, \tag{44}$$

$$x'(x,t) = \sum_{m=1}^{M_r} x_{1m}(x,t) + 2\sum_{m=1}^{M_c} \mathrm{Re}\{z_{1m}(x,t)\}, \tag{45}$$

$$x_{1m}(x,t) = A_m i(x,t-\Delta t) + a_m x_{2n}(x,t-\Delta t), \tag{46}$$

$$z_{1m}(x,t) = B_m i(x,t-\Delta t) + b_m z_{2m}(x,t-\Delta t), \tag{47}$$

$$x_{2m}(x,t) = A_m i(x,t) + x_{1m}(x,t), \tag{48}$$

$$z_{2m}(x,t) = B_m i(x,t) + z_{1m}(x,t). \tag{49}$$

Here, Δt is the computation time step and A_m, a_m, B_m, and b_m are the coefficients determined by the real/image poles and their residues of the rational function $H(j\omega)$, which is an approximation of the ground impedance in the frequency domain

$$H(j\omega) \cong \sum_{m=1}^{M_r} \frac{R_m}{j\omega - p_m} + \sum_{m=1}^{M_c} \frac{\hat{R}_m}{j\omega - \hat{p}_m} + \frac{\hat{R}_m^*}{j\omega - \hat{p}_m^*} \tag{50}$$

$$A_m = \frac{R_m}{2/\Delta t - p_m},\ a_m = \frac{2/\Delta t + p_m}{2/\Delta t - p_m} \tag{51}$$

$$B_m = \frac{\hat{R}_m}{2/\Delta t - \hat{p}_m},\ b_m = \frac{2/\Delta t + \hat{p}_m}{2/\Delta t - \hat{p}_m}. \tag{52}$$

In (50), the symbol * denotes the complex conjugate.

2) FDTD Method for Solving Agrawal et al. Formula: The Agrawal et al. formula given by (41) and (43) is solved using the point-centered FDTD method. The scattered voltage and the total current are allocated alternatively along the line. The voltage at the kth node of the Pi-equivalent is denoted as v_k, and the current at the center of the Pi-equivalent is denoted as $i_{k+1/2}$. Furthermore, they are allocated alternatively in the time domain; the voltage v_k^n is allocated at $t = n\Delta t$ ($n = 0, 1, 2, \ldots$) and the current $i_{k+1/2}^{n+1/2}$ is allocated at $t = (n+1/2)\Delta t$. The above allocations can be expressed as the equivalent circuit shown in

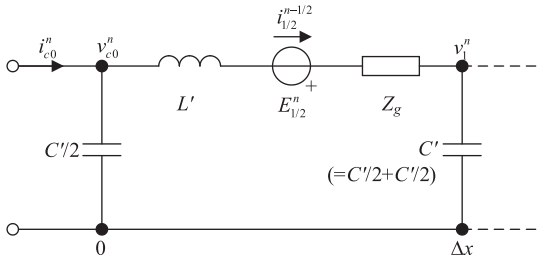

Fig. 7. Connecting point of Agrawal et al. formula and EMT analysis (leftmost node).

Fig. 6, and update equations of the voltage and current are

$$v_k^n = v_k^{n-1} - \frac{\Delta t}{\Delta x} C'^{-1} \left(i_{k-1/2}^{n-1/2} - i_{k-1/2}^{n-1/2} \right), \tag{53}$$

$$\begin{aligned} i_{k+1/2}^{n+1/2} = & -\left(\frac{H_0}{2} + \frac{L'}{\Delta t} \right)^{-1} \left(\frac{H_0}{2} - \frac{L'}{\Delta t} \right) i_{k+1/2}^{n-1/2} \\ & - \left(\frac{H_0}{2} + \frac{L'}{\Delta t} \right)^{-1} \left(x'^{n+1/2}_{k+1/2} + x'^{n-1/2}_{k+1/2} \right) \\ & - \frac{1}{\Delta x} \left(\frac{H_0}{2} + \frac{L'}{\Delta t} \right)^{-1} \left(v_k^n - v_{k-1}^n \right) \\ & + \left(\frac{H_0}{2} + \frac{L'}{\Delta t} \right)^{-1} E_{k+1/2}^n \end{aligned} \tag{54}$$

where $E_{k+1/2}^n$ is the incident horizontal electric field at $t = n\Delta t$ and $x'^{n+1/2}_{k+1/2}$ is obtained as follows:

$$x'^{n+1/2}_{k+1/2} = \sum_{m=1}^{M_r} x^{n+1/2}_{1m\,k+1/2} + 2 \sum_{m=1}^{M_c} \mathrm{Re} \left\{ z^{n+1/2}_{1m\,k+1/2} \right\}, \tag{55}$$

$$x^{n-1/2}_{1m\,k+1/2} = A_m i^{n-1/2}_{k+1/2} + a_m x^{n-1/2}_{2n\,k+1/2}, \tag{56}$$

$$z^{n+1/2}_{1m\,k+1/2} = B_m i^{n-1/2}_{k+1/2} + b_m z^{n-1/2}_{2m\,k+1/2}, \tag{57}$$

$$x^{n+1/2}_{2m\,k+1/2} = A_m i^{n+1/2}_{k+1/2} + x^{n+1/2}_{1m\,k+1/2}, \tag{58}$$

$$z^{n+1/2}_{2m\,k+1/2} = B_m i^{n+1/2}_{k+1/2} + z^{n+1/2}_{1m\,k+1/2}. \tag{59}$$

3) Interface of Agrawal et al. Formula and EMT Analysis: The Agrawal et al. formula and the EMT analysis are interfaced by considering the presence of a distributed capacitance at both ends of the Pi-equivalent. Fig. 7 shows the connecting point of the Agrawal et al. formula and the EMT analysis. At the leftmost node, the following relation is satisfied:

$$i_{1/2}^{n-1/2} - i_{c0}^{n-1/2} = -\frac{C'}{2} \frac{\Delta x}{2} \frac{\left(v_{c0}^n - v_{c0}^{n-1} \right)}{\Delta t} \tag{60}$$

where v_{c0}^n is the total voltage of the leftmost node (and at the same time, the node voltage in the EMT analysis) and $i_{c0}^{n-1/2}$ is the current in the EMT analysis. By approximating $i_{c0}^{n-1/2} = (i_{c0}^n + i_{c0}^{n-1})/2$, the equation for calculating i_{c0}^n can be derived as follows:

$$i_{c0}^n = G_c v_{c0}^n + J_{c0}^n \tag{61}$$

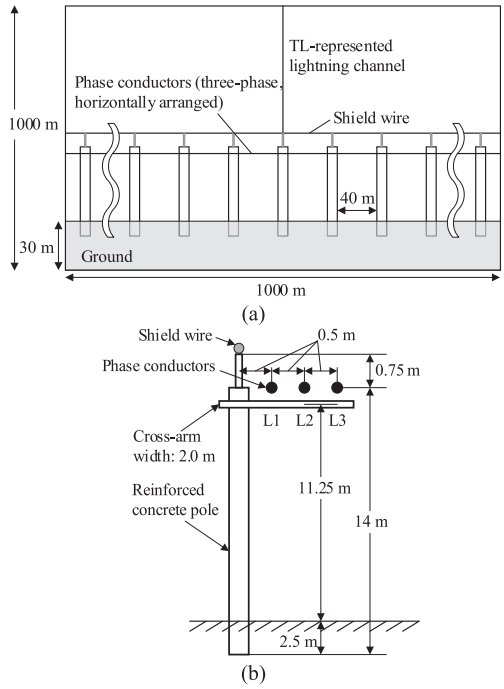

Fig. 8. FDTD calculation model of distribution line (not in scale). (a) Side view of FDTD analysis space. (b) Arrangement of pole and conductors.

where

$$G_c = \frac{C'\Delta x}{2\Delta t}, J_{c0}^n = -G_c v_{c0}^{n-1} + 2 \left(i_{1/2}^{n-1/2} - \frac{i_{c0}^{n-1}}{2} \right). \tag{62}$$

A similar expression for the current at the rightmost node can be derived. The Agrawal et al. formula and the EMT analysis are interfaced by the equivalent conductance G_c and the current sources containing the histories J_{c0} at the leftmost node and J_{cK} at the rightmost node.

III. Application of the Proposed Method for Analyzing Direct Lightning Strike to Distribution Lines

A. Analysis by the 3-D FDTD Method

The 3-D FDTD model of a lightning strike to a distribution pole was composed. Fig. 8 shows the FDTD analysis space and the configuration of the distribution pole. The FDTD analysis space of 1000 m × 400 m × 1000 m was divided into cubic cells with a minimum side length of 0.125 m and a maximum side length of 5 m, with a total of 798 × 161 × 355 cells. The bottom 30 m was set as ground with a resistivity of 100 Ωm and a relative permittivity of 10. Boundaries were treated by the second-order Liao's absorbing boundary [33].

The concrete pole was modeled by a rectangular conductor of 14 m length and 0.25 m width, and the bottom 2.5 m was buried inside the ground. A 0.75-m-long metal frame for the shield wire was also modeled. The radii of the shield wire and phase conductors were 3 and 5.8 mm, respectively. They were modeled by the thin-wire representation method by modifying the permeability and permittivity around the conductor [34]. The phase conductors L1, L2, and L3 were arranged as shown in

Fig. 8(b). The cross-arm was modeled by a rectangular conductor of 2 m length and 0.05 m width. The insulator voltage was defined by the electric field between the phase conductor and the cross-arm. The span length was set to 40 m. Both ends of the shield wire and phase conductors were attached to the absorbing boundary to suppress reflections of the traveling voltage and current. The lightning channel was represented by the transmission line model with a lightning current traveling speed of 100 m/μs. The base of the channel was connected to the top of the distribution pole. The current representing the first and subsequent strokes expressed by Heidler's function [35] used in [15] was considered.

B. Analysis by Proposed Method

The analysis model for a direct lightning strike was synthesized by the proposed method. The concrete pole was represented by a lossless distributed-parameter line model with a height of 15 m, a surge impedance of 300 Ω, and a traveling wave speed of c_0; the grounding was modeled by a resistance of 20 Ω [15]. Neither the frequency nor the current-dependent characteristic of the grounding was considered. Both ends of the overhead conductors were terminated by multiphase matching circuits. The spatial step Δx for solving the Agrawal et al. formula was set to 1 m. Note that in considering the effect of imperfectly conducting ground on the horizontal electric fields, the Cooray–Rubinstein formula [36], [37] was used. The magnetic field required in the Cooray–Rubinstein formula can be derived in the same manner as the electric field.

In the proposed method, the incident voltage of the shield wire, $v^i_{\rm sw}$, at the struck point cannot be calculated since the denominator of (1) becomes zero. Hence, this incident voltage was calculated using voltages v^i_1–v^i_3 in the vicinity. We defined the position of $v^i_{\rm sw}$ as $(x_{\rm sw}, y_{\rm sw}, z)$ and those of v^i_1–v^i_3 as $(x_{\rm sw}, y_1, z)$, $(x_{\rm sw}, y_2, z)$, and $(x_{\rm sw}, y_3, z)$, respectively. By interpolation, the incident voltage $v^i_{\rm sw}$ can be calculated as follows:

$$v^i_{\rm sw} = \frac{(y_{\rm sw}-y_2)(y_{\rm sw}-y_3)}{(y_1-y_2)(y_1-y_3)}v^i_1 + \frac{(y_{\rm sw}-y_1)(y_{\rm sw}-y_3)}{(y_2-y_1)(y_2-y_3)}v^i_2 + \frac{(y_{\rm sw}-y_1)(y_{\rm sw}-y_2)}{(y_3-y_1)(y_3-y_2)}v^i_3. \quad (63)$$

The analysis was also performed by the method only considering the LEMPs from the lightning channel, as well as by EMT analysis without considering the LEMPs. The same models as those in the proposed method were used to represent the distribution poles and the grounding.

C. Results and Discussion

The insulator voltages computed by each method are shown in Fig. 9. The proposed method as well as the method only considering the LEMPs from the lightning channel can roughly reproduce the insulator voltages computed by the 3-D FDTD method, while the EMT analysis not considering the LEMP effect provides much lower insulator voltages. This is because the methods considering the LEMPs can take into account the voltages on the shield wire and phase conductors induced by the LEMPs, which have the opposite polarity from the voltages generated by the current flowing into the shield wires and the distribution pole struck by lightning [15].

The difference between the proposed method and the 3-D FDTD method can be attributed to the modeling of the distribution pole. In this article, as mentioned in Section III-B, the distribution pole is modeled by a lossless distributed-parameter line with a surge impedance of 300 Ω and the wave traveling speed of c_0 following [15]. The surge impedance of 300 Ω was determined on the basis of the peak value of the pole-top voltage divided by the pole-top current measured in an experiment, in which the step-like current was injected into the distribution pole top [38]. The lossless line is a simple expression for representing distribution poles. However, it is known that the surge impedance of vertical objects, such as distribution poles and transmission towers, increases with time owing to electromagnetic field formation and that the traveling wave along the object suffers a significant attenuation [39]. Thus, the modeling of the distribution pole adopted in this study provides higher insulator voltages generated by the subsequent stroke current and lower insulator voltages generated by the first stroke current (besides, overoscillation characteristics for the subsequent stroke).

The method only considering the LEMPs from the lightning channel provided more similar voltages to the 3-D FDTD method than the proposed method. This result can be attributed to the contribution of the simple concrete pole model and the ignoring of LEMPs from the struck pole: these effects were balanced to provide accurate voltages. In addition, the LEMPs have less impact for a 10-m-high distribution pole than for a 100-m-high object, as shown in Appendix A. Note that for the method only considering the LEMPs from the lightning channel, the use of an accurate distribution pole model can result in inaccurate insulator voltages.

The accuracy of the proposed method can be improved by modeling the distribution pole more precisely, while that of the method only considering the LEMPs from the lightning channel deteriorates. The following is an example of an improvement of the pole model. Fig. 10 shows the insulator voltages computed by each method using an improved model of the concrete pole struck by lightning. In the improved pole model, the surge impedance was set as time-dependent; its step-current response has an initial value of 150 Ω and a convergence value of 300 Ω with a time constant of 1 μs. This time-dependent surge impedance approximately represents the electromagnetic field formation. The grounding of the distribution pole was modeled by a series circuit with a grounding resistance of 20 Ω and a resistance R_t–inductance L_t parallel circuit. The R_t–L_t parallel circuit approximately represents the significant wave attenuation along the distribution pole. The resistance R_t was set to 60 Ω following [40]. The inductance L_t was set to 300 μH (a time constant of 5 μs for the R_t–L_t parallel circuit) since the effect of attenuation can be observed in the period around 5 μs or later, as shown in Fig. 9(a-2) and (b-2). As shown in Fig. 10, the proposed method with the improved distribution pole model can provide insulator voltages similar to those of the 3-D FDTD

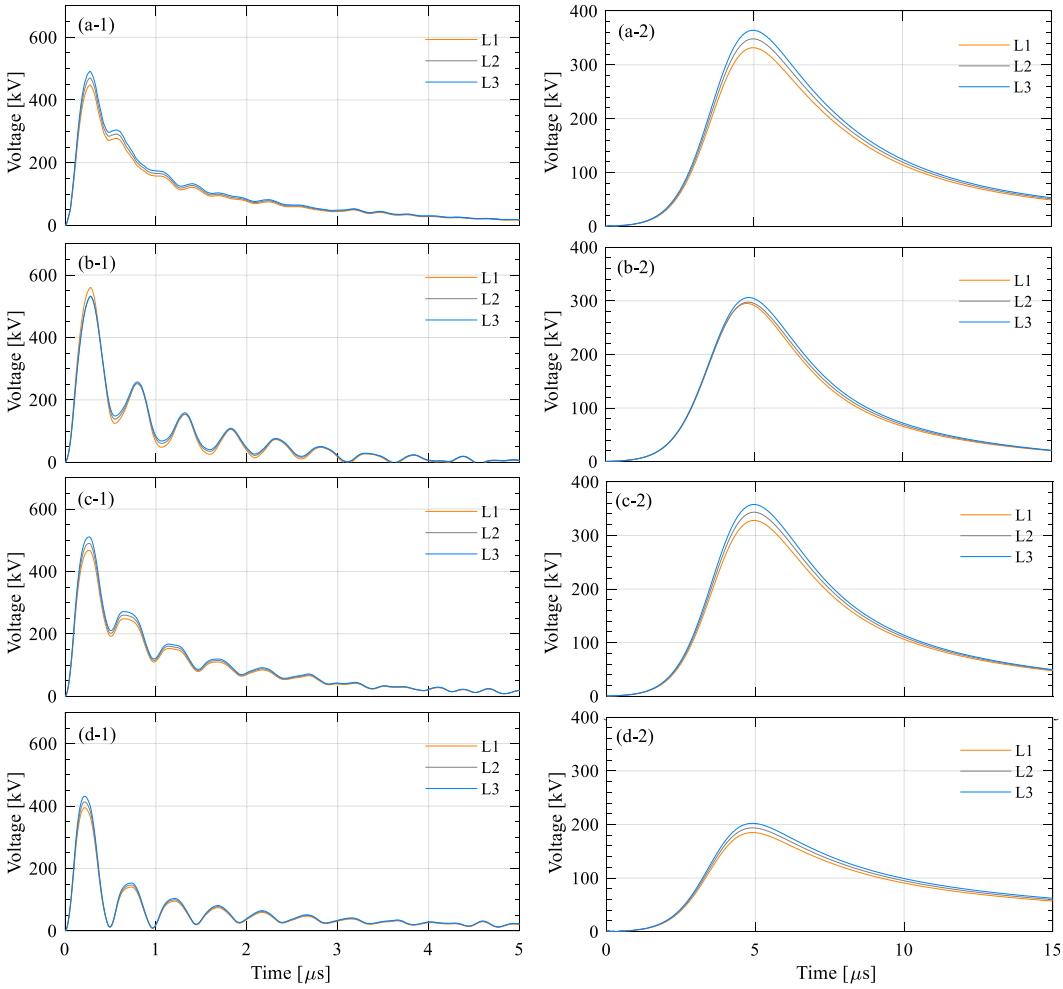

Fig. 9. Insulator voltages generated by (1) subsequent and (2) first stroke currents computed by (a) 3-D FDTD method, (b) proposed method considering LEMPs from lightning channel and struck pole, (c) method only considering LEMPs from lighting channel, and (d) EMT analysis not considering LEMPs.

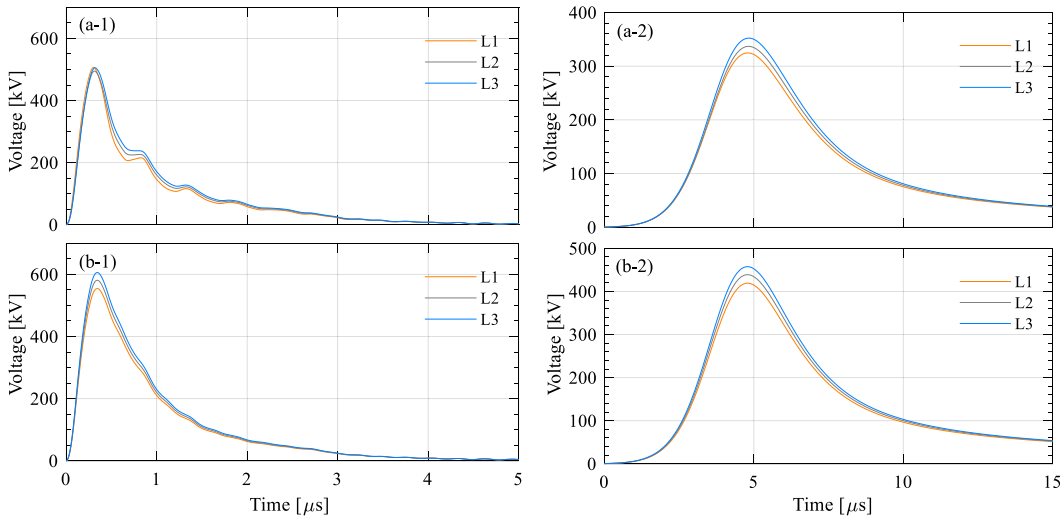

Fig. 10. Insulator voltages calculated using improved model of distribution pole computed by (a) proposed method considering LEMPs from lightning channel and struck pole, and (b) method only considering LEMPs from lightning channel. Note that the vertical axis of (b-2) is different from that of (a-2) of this figure and (a-2) to (d-2) of Fig. 9.

method, whereas the method only considering the LEMPs from the lightning channel provides higher insulator voltages in both current waveforms.

As shown above, if the concrete pole is modeled with its characteristics considered precisely, the proposed method, which considers the LEMPs from the lightning channel and the struck pole, provides accurate insulator voltages. On the other hand, if the simple concrete pole model is used, the method only considering the LEMP from the lightning channel provides accurate insulator voltages. Note that the rather simpler representation of the distribution poles, such as that by an inductor, can also provide accurate insulator voltages for the first stroke current.

The proposed method is fast and can be used for evaluating the lightning performance of distribution lines with multiple calculations. For example, the proposed method takes 42 s to derive the 10-μs long transient response while the FDTD method takes 38 810 s, with 3.0 GHz Intel i7 4-cores CPU, 32 GB of RAM running Windows 10. The OpenMP [41] was used to accelerate the computation for both methods. Note that the FDTD method is suitable for parallel computation, and for example, the calculation time can be shortened to 2489 s by NEC's Vector Engine Processor SX-Aurora TSUBASA [42]. The proposed method is still much faster than the FDTD method and can be run in a standard desktop environment. Therefore, the proposed method can become a useful tool for statistically assessing the lightning performance of distribution lines.

IV. Conclusion

We proposed an analysis method for a direct lightning strike to overhead distribution lines that considers the effect of LEMPs from a lightning channel and a pole struck by lightning. The LEMPs were computed using the scalar and vector potential formulae, which were extended to include the presence of the struck pole, using the current flowing into the lightning channel, the pole top, and the pole base. The effect of the LEMPs on the overhead conductors was considered by the Agrawal et al. formula. This formula was solved by the point-centered FDTD method, and it was interfaced with EMT analysis considering the distributed capacitance at both ends of the line: the entire transient analysis can be performed within the EMT analysis. The proposed method with an accurate concrete pole model can provide voltages similar to those of the 3D-FDTD method. If the simple model is used for the concrete pole, the method only considering the LEMPs from the lightning channel provides insulator voltages similar to those of the 3-D FDTD method. The proposed method developed on the basis of the transmission-line theory is expected to be a useful tool for statistically assessing the lightning performance of distribution lines.

Appendix

A. Validation of the Proposed Method by Calculation of Lightning-Induced Voltage

In addition to the case of a direct lightning strike, the proposed method was validated by referencing a calculation of the voltage induced by a lightning strike to a tall object located near an overhead conductor presented in [43]. At the same time, the effect of LEMPs radiated from the struck object was evaluated.

In the calculation, a lightning strike to a 100-m-high object was assumed, and the induced voltage at the center of a 10-m-high, 1200-m-long, and 5-mm-radius overhead conductor was calculated by the 3-D FDTD method. The distance between the tall object and the center of the conductor, d, was set to 40, 60, 100, and 200 m. The reflection coefficients at the top and base of the struck object, $\rho_{\rm tot}$ and $\rho_{\rm bot}$, were set to -0.5 and 1, respectively. These reflection coefficients correspond to values of 900, 300, and 0 Ω for the lightning channel impedance, tall-object surge impedance, and tall-object grounding impedance, respectively. The current distributions along the lightning channel and the struck object were computed using the "engineering" TL model, which has been extended to include a tall object [44]. The current traveling speeds along the channel and the object were set to $c_0/3$ and c_0, respectively. Both ends of the overhead conductor were terminated by a matching resistance of 498 Ω. The resistivity and permittivity of the ground were set to 100 Ωm and 10, respectively.

The above-described system was synthesized by the proposed method as well as the method only considering the LEMPs from the lightning channel. The spatial step for solving the Agrawal et al. coupling formula was set to 1 m.

The proposed method reproduced the voltages computed by the 3-D FDTD method shown in [41]. Fig. 11 shows the induced voltages at the center of the conductor for each distance between the conductor and the tall object. The voltage waveforms, including their peaks and the oscillating characteristic resulting from the traveling wave reflection at the top and base of the tall object, were accurately computed by the proposed method. The results validated the proposed method for the LEMP calculation that considers the lightning channel and the struck object using the potential formulae as well as the induced voltage calculation.

Fig. 11(c) shows the voltages computed considering the LEMPs radiated from the lightning channel only. In this case, the oscillating characteristic appeared owing to the traveling current flowing into the lightning channel from the top of the object. However, the voltage peaks are much lower than those derived by the 3-D FDTD method. The LEMP from the struck object has a significant impact in this case.

B. Discussion on Method Assuming Lightning Strike to Flat Ground Away From Struck Pole

In this appendix, we discuss the method of direct lightning surge analysis assuming a lightning strike to flat ground away from the struck pole [12], [13], [14], [15]. We show that this method provides similar voltages to the 3-D FDTD method owing to the contributions of some factors and that it is necessary to examine the validity of computed voltages by using, for instance, 3-D FDTD analysis results in advance of the lightning performance assessment.

For the discussion, an analysis model was synthesized following [15]. The models for the concrete pole and grounding were the same as those described in Section III-B: a surge impedance of 300 Ω and a traveling wave speed of c_0 for the concrete pole

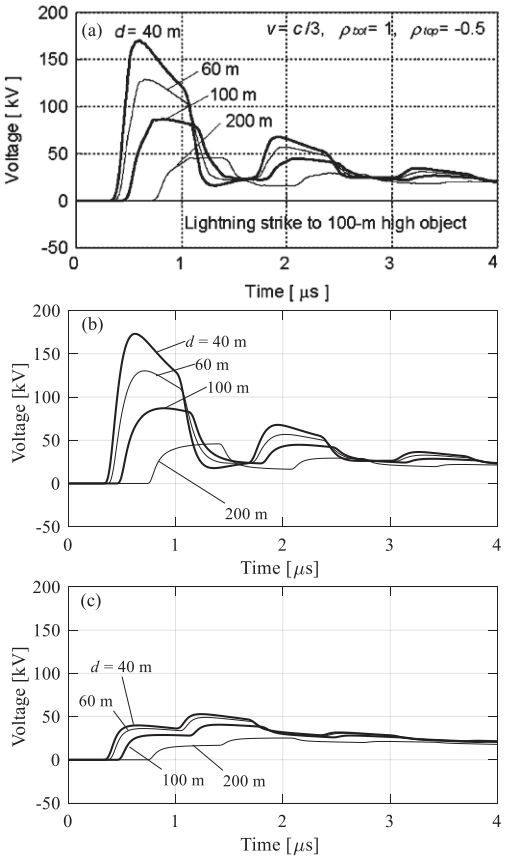

Fig. 11. Lightning-induced voltages at center point of horizontal wire at distances $d = 40$, 60, 100, and 200 m from struck object calculated by (a) FDTD method (adopted from [43]), (b) proposed method considering the LEMPs from lightning channel and struck object, and (c) method only considering LEMPs from lightning channel.

and a linear resistance of 20 Ω for the grounding. The lightning channel was placed 10 m from the struck pole on the side of conductor L3 (Fig. 8 showed the arrangement).

Fig. 12 shows the insulator voltages derived by the method. Compared with the voltages derived by the FDTD method shown in Fig. 9(a-1) and (a-2), higher voltages are derived for the subsequent stroke and similar voltages are derived for the first stroke, respectively, by the method of direct lightning surge analysis assuming a lightning strike to flat ground away from the struck pole. This method provides different voltages among conductors L1–L3, especially for the subsequent stroke, since the lightning strike to flat ground 10 m from the pole on the side of conductor L3 was considered. The voltage induced by the LEMP becomes maximum in conductor L3, where the mutual surge impedances of shield wire and phase conductors are minimum (in other words, the voltages generated by the current flowing into the pole and shield wires become maximum).

The method assuming a lightning strike to flat ground away from the struck pole provides similar electric fields to the proposed method assuming a lightning strike to the distribution pole. Fig. 13 shows the incident horizontal electric field and Fig. 14 shows the incident voltage computed by each method.

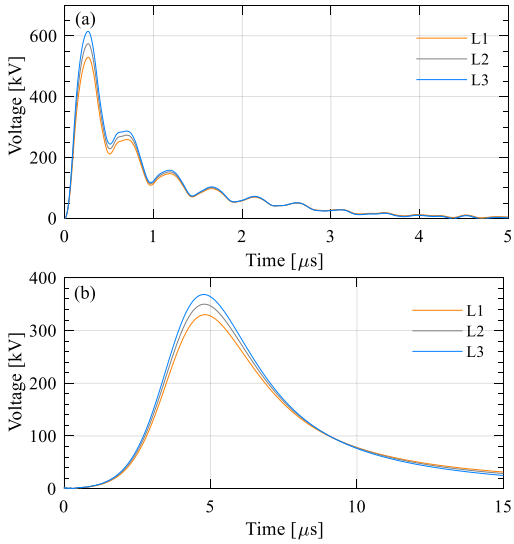

Fig. 12. Insulator voltages computed by assuming lightning strike to flat ground 10 m from struck pole for LEMP calculation. (a) Subsequent stroke and (b) first stroke. These voltages should be compared with those in Fig. 9(a-1) and (a-2).

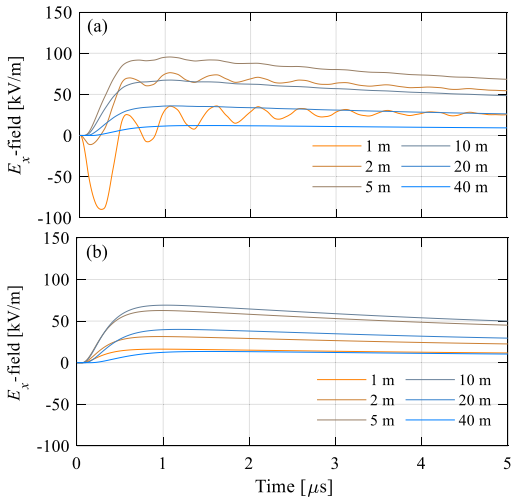

Fig. 13. Incident horizontal electric field waveforms of conductor L1 calculated by assuming (a) lightning strike to pole (proposed method) and (b) lightning strike to flat ground 10 m from pole (method used in [12], [13], [14], [15]). Waveforms for the subsequent stroke are shown.

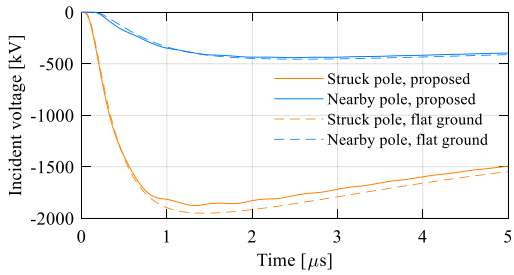

Fig. 14. Incident voltage waveforms of conductor L1 at struck pole and nearby pole calculated by assuming (a) lightning strike to pole (proposed method) and (b) lightning strike to flat ground 10 m from pole (method used in [12], [13], [14], [15]). Waveforms for the subsequent stroke are shown.

In the fields computed by the proposed method, the effect of traveling wave reflection inside the pole can be observed as an oscillating waveform. However, the oscillation characteristic disappears at around 20 m from the pole, and each method provides similar waveforms. Similar characteristics were derived for the first stroke. The LEMPs computed by the method assuming a lightning strike to flat ground away from the struck pole are a good approximation of those computed assuming a lightning strike to the distribution pole.

The method assuming a lightning strike to flat ground away from the struck pole provides similar results to the 3-D FDTD method owing to the following factors:

1) the lightning channel was placed on the side of conductor L3 where the insulator voltage becomes maximum;
2) the LEMPs computed by this channel were similar to those computed for a lightning strike to the distribution pole;
3) as discussed in Section III-C, the concrete pole model had a characteristic that provides higher insulator voltages for the subsequent stroke and lower insulator voltages for the first stroke.

Therefore, although the method assuming a lightning strike to flat ground away from the struck pole is quite practical, it requires validation, for instance, by using the 3-D FDTD method, in advance of the lightning performance assessment of distribution lines.

Acknowledgment

The authors would like to thank Prof. C. A. Nucci, Prof. A. Borghetti, Prof. F. Napolitano, and Prof. F. Tossani of University of Bologna for their valuable comments.

References

[1] A. Borghetti, C. A. Nucci, and M. Paolone, "An improved procedure for the assessment of overhead line indirect lightning performance and its comparison with the IEEE Standard 1410 method," *IEEE Trans. Power Del.*, vol. 22, no. 1, pp. 684–692, Jan. 2007.

[2] A. Borghetti, F. Napolitano, C. A. Nucci, and F. Tossani, "Influence of the return stroke current waveform on the lightning performance of distribution lines," *IEEE Trans. Power Del.*, vol. 32, no. 4, pp. 1800–1808, Aug. 2017.

[3] S. Oguchi, T. Ishii, S. Okabe, Y. Sakamoto, M. Tsuji, and A. Asakawa, "Observational and experimental study of the lightning stroke attraction effect with ground wire system constructions," *IEEE Trans. Dielect. Elect. Insul.*, vol. 19, no. 1, pp. 363–370, Feb. 2012.

[4] J. Cao et al., "Comprehensive assessment of lightning protection schemes for 10 kV overhead distribution lines," *IEEE Trans. Power Del.*, vol. 37, no. 3, pp. 2326–2336, Jun. 2022.

[5] K. Nakada et al., "Energy absorption of surge arresters on power distribution lines due to direct lightning strokes-effects of an overhead ground wire and installation position of surge arresters," *IEEE Trans. Power Del.*, vol. 12, no. 4, pp. 1779–1785, Oct. 1997.

[6] T. Miyazaki and S. Okabe, "Experimental investigation to calculate the lightning outage rate of a distribution system," *IEEE Trans. Power Del.*, vol. 25, no. 4, pp. 2913–2922, Oct. 2010.

[7] A. Takahashi, S. Furukawa, K. Ishimoto, A. Asakawa, and T. Hidaka, "Influence of grounding resistance on effectiveness of lightning protection for power distribution lines with surge arresters," in *Proc. 30th Int. Conf. Lightning Protection*, 2010, pp. 1–6.

[8] K. Michishita and Y. Hongo, "Flashover rate of 6.6-kV distribution line due to direct negative lightning return strokes," *IEEE Trans. Power Del.*, vol. 27, no. 4, pp. 2203–2210, Oct. 2012.

[9] P. N. Mikropoulos and T. E. Tsovilis, "Statistical method for the evaluation of the lightning performance of overhead distribution lines," *IEEE Trans. Dielect. Elect. Insul.*, vol. 20, no. 1, pp. 202–211, Feb. 2013.

[10] J. Chen and M. Zhu, "Calculation of lightning flashover rates of overhead distribution lines considering direct and indirect strokes," *IEEE Trans. Electromagn. Compat.*, vol. 56, no. 3, pp. 668–674, Jun. 2014.

[11] E. Stracqualursi, R. Araneo, and A. Andreotti, "Preliminary assessment of protection of distribution lines against direct lightning strokes through multi-chamber arresters and shield wires," in *Proc. IEEE Int. Conf. Environ. Elect. Eng. IEEE Ind. Commercial Power Syst. Europe*, 2022, pp. 1–5.

[12] F. Tossani et al., "Estimation of the influence of direct strokes on the lightning performance of overhead distribution lines," in *Proc. IEEE Eindhoven PowerTech*, 2015, pp. 1–7.

[13] A. Borghetti, F. Napolitano, C. A. Nucci, and F. Tossani, "Response of distribution networks to direct and indirect lightning: Influence of surge arresters location, flashover occurrence and environmental shielding," *Electric Power Syst. Res.*, vol. 153, pp. 73–81, Dec. 2017.

[14] A. Borghetti, K. Ishimoto, F. Napolitano, C. A. Nucci, and F. Tossani, "Assessment of the effects of the electromagnetic pulse on the response of overhead distribution lines to direct lightning strikes," *IEEE Open Access J. Power Energy*, vol. 8, pp. 522–531, 2021.

[15] K. Ishimoto, F. Tossani, F. Napolitano, A. Borghetti, and C. A. Nucci, "Direct lightning performance of distribution lines with shield wire considering LEMP effect," *IEEE Trans. Power Del.*, vol. 37, no. 1, pp. 76–84, Feb. 2022.

[16] J. Cao et al., "Lightning surge analysis of transmission line towers with a hybrid FDTD-PEEC method," *IEEE Trans. Power Del.*, vol. 37, no. 2, pp. 1275–1284, Apr. 2022.

[17] "EMTP home," 2022. Accessed: May 25, 2022. [Online]. Available: https://www.emtp.com/

[18] K. Yee, "Numerical solution of initial boundary value problems involving Maxwell's equations in isotropic media," *IEEE Trans. Antennas Propag.*, vol. 14, no. 3, pp. 302–307, May 1966.

[19] A. Tatematsu, "Development of a surge simulation code VSTL REV based on the 3D FDTD method," in *Proc. IEEE Int. Symp. Electromagn. Compat.*, 2015, pp. 1111–1116.

[20] F. Napolitano, A. Borghetti, C. A. Nucci, M. Paolone, F. Rachidi, and J. Mahseredjian, "An advanced interface between the LIOV code and the EMTP-RV," in *Proc. 29th Int. Conf. Lightning Protection*, 2008, vol. 1, pp. 1–12.

[21] A. Borghetti, W. A. Chisholm, F. Napolitano, C. A. Nucci, F. Rachidi, and F. Tossani, "Software tools for the lightning performance assessment," in *Lightning Interaction With Power Systems Vol. 2: Applications*, A. Piantini, Ed. London, U.K.: IET, 2020, pp. 425–452.

[22] S. Sekioka, T. Nagai, Y. Sonoi, and I. Matsubara, "A computation method of voltages across insulator strings considering the effect of lightning strokes," *IEEJ Trans. Power Energy*, vol. 114, no. 4, pp. 373–380, 1994.

[23] T. Sonoda, H. Morii, and S. Sekioka, "Observation of lightning overvoltage in a 500 kV switching station," *IEEE Trans. Power Del.*, vol. 32, no. 4, pp. 1828–1834, Aug. 2017.

[24] A. Sakakibara, "Calculation of induced voltages on overhead lines caused by inclined lightning studies," *IEEE Trans. Power Del.*, vol. 4, no. 1, pp. 683–693, Jan. 1989.

[25] A. K. Agrawal, H. J. Price, and S. H. Gurbaxani, "Transient response of multiconductor transmission lines excited by a nonuniform electromagnetic field," *IEEE Trans. Electromagn. Compat.*, vol. 22, no. 2, pp. 119–129, May 1980.

[26] G. Hachtel, R. Brayton, and F. Gustavson, "The sparse tableau approach to network analysis and design," *IEEE Trans. Circuit Theory*, vol. 18, no. 1, pp. 101–113, Jan. 1971.

[27] H. W. Dommel, "Digital computer solution of electromagnetic transients in single-and multiphase networks," *IEEE Trans. Power App. Syst.*, vol. PAS-88, no. 4, pp. 388–399, Apr. 1969.

[28] V. Cooray, "Calculating lightning-induced overvoltages in power lines. A comparison of two coupling models," *IEEE Trans. Electromagn. Compat.*, vol. 36, no. 3, pp. 179–182, Aug. 1994.

[29] E. D. Sunde, *Earth Conduction Effects in Transmission Systems*, New York, NY, USA: Dover Publications, Inc., 1968.

[30] F. Rachidi, C. A. Nucci, and M. Ianoz, "Transient analysis of multiconductor lines above a lossy ground," *IEEE Trans. Power Del.*, vol. 14, no. 1, pp. 294–302, Jan. 1999.

[31] T. Noda, "MATLAB source code: Frequency-partitioning fitting method for linear equivalent identification from frequency response data," IEEE data port, Jul. 14, 2019. Accessed: Jun. 21, 2022. [Online]. Available: https://ieee-dataport.org/documents/matlab-source-code-frequency-partitioning-fitting-method-linear-equivalent-identification

[32] T. Noda, "Identification of a multiphase network equivalent for electromagnetic transient calculations using partitioned frequency response," *IEEE Trans. Power Del.*, vol. 20, no. 2, pp. 1134–1142, Apr. 2005.

[33] Z. P. Liao, H. L. Wong, B. P. Yang, and Y. F. Yuan, "A transmitting boundary for transient wave analysis," *Sci. Sin.*, vol. A27, no. 10, pp. 1063–1076, Oct. 1984.
[34] T. Noda and S. Yokoyama, "Thin wire representation in finite difference time domain surge simulation," *IEEE Trans. Power Del.*, vol. 19, no. 3, pp. 840–847, Jul. 2002.
[35] F. Heidler, "Analytische blitzstromfunktion zur LEMP-berechnung," in *Proc. 18th Int. Conf. Lightning Protection*, 1985, pp. 63–66.
[36] V. Cooray, "Horizontal fields generated by return strokes," *Radio Sci.*, vol. 27, no. 4, pp. 529–537, 1992.
[37] M. Rubinstein, "An approximate formula for the calculation of the horizontal electric field from lightning at close, intermediate, and long range," *IEEE Trans. Electromagn. Compat.*, vol. 38, no. 3, pp. 531–535, Aug. 1996.
[38] S. Matsuura, A. Tatematsu, T. Noda, and S. Yokoyama, "A simulation study of lightning surge characteristics of a distribution line using the FDTD method," *IEEJ Trans. Power Energy*, vol. 129, no. 10, pp. 1225–1232, 2009.
[39] A. Yamanaka, N. Nagaoka, and Y. Baba, "Circuit model of vertical double-circuit transmission tower and line for lightning surge analysis considering TEM-mode formation," *IEEE Trans. Power Del.*, vol. 35, no. 5, pp. 2471–2480, Oct. 2020.
[40] S. Matsuura, T. Noda, A. Asakawa, and S. Yokoyama, "Lightning surge characteristics of an actual distribution line and validation of a distribution line model for lightning overvoltage studies," *IEEJ Trans. Power Energy*, vol. 128, no. 9, pp. 1150–1158, 2008.
[41] "Home - OpenMP," 2023. Accessed: May 17, 2023. [Online]. Available: https://www.openmp.org/
[42] "NEC's vector engine processor SX aurora TSUBASA," 2023. Accessed: May 17, 2023. [Online]. Available: https://www.necam.com/VectorEngineProcessor/
[43] Y. Baba and V. A. Rakov, "Voltages induced on an overhead wire by lightning strikes to a nearby tall grounded object," *IEEE Trans. Electromagn. Compat.*, vol. 48, no. 1, pp. 212–224, Feb. 2006.
[44] Y. Baba and V. A. Rakov, "On the use of lumped sources in lightning return stroke models," *J. Geophysical Res., Atmos.*, vol. 110, no. D3, 2005. [Online]. Available: https://agupubs.onlinelibrary.wiley.com/doi/full/10.1029/2004JD005202

Akifumi Yamanaka (Member, IEEE) received the B.Sc., M.Sc., and Ph.D. degrees in electrical engineering all from Doshisha University, Kyoto, Japan, in 2017, 2019, and 2021, respectively.

In 2021, he joined the Central Research Institute of Electric Power Industry (CRIEPI), Yokosuka, Japan. His research interests include numerical electromagnetic and EMT analysis of lightning phenomena, and lightning protection of transmission and distribution systems.

Dr. Yamanaka was the recipient of the International Conference on Power Systems Transients (IPST) Young Scientist Award in 2023. He is a member of the Institute of Electrical Engineers of Japan, the Institute of Electrical Installation Engineers of Japan, and the International Council of Large Electric Systems (CIGRE).

Kazuyuki Ishimoto (Member, IEEE) received the B.S., M.S., and Ph.D. degrees in electrical engineering from Waseda University, Tokyo, Japan, in 2007, 2009 and 2018, respectively.

Since 2009, he has been with the Central Research Institute of Electric Power Industry, Yokosuka, Japan. He was a Visiting Researcher of the Power Systems Laboratory at the University of Bologna, Bologna, Italy, from 2019 to 2020. His research interests include the area of high voltage, with particular to lightning protection of power systems.

Dr. Ishimoto was the recipient of the International Conference on Lightning Protection Young Scientists Awards in 2016. He is currently the Secretary of C4.57 Workings Group of the International Council of Large Electric Systems (CIGRE).

Akiyoshi Tatematsu (Senior Member, IEEE) received the B.E., M.E., and Ph.D. degrees in electrical engineering from Kyoto University, Kyoto, Japan, in 1999, 2001, and 2004, respectively.

He has been with the Central Research Institute of Electric Power Industry, Yokosuka, Japan, since 2004. He was a Postdoctoral Fellow of the Electromagnetic Compatibility Laboratory, Swiss Federal Institute of Technology, Lausanne, Switzerland, from 2012 to 2013. His research interests include the study of numerical electromagnetic field analysis, electromagnetic transient analysis, and lightning protection of electric power facilities.

Dr. Tatematsu is a Distinguished Reviewer of IEEE TRANSACTIONS ON ELECTROMAGNETIC COMPATIBILITY in 2014, 2015, 2019–2022. He was the recipient of the International Conference on Lightning Protection Diploma for Young Scientists in 2006 and 2010. He is currently the Chairperson of Japanese National Committee for IEC SC77C and the Secretaries of C4.43 and C4.54 Workings Group of the International Council of Large Electric Systems (CIGRE). He is a member of the IEEJ and CIGRE.